Contents lists available at *Dergipark*

Journal of Scientific Reports-A

journal homepage: *https://dergipark.org.tr/tr/pub/jsr-a*

E-ISSN: 2687-6167 ***Number 61, June 2025***

RESEARCH ARTICLE

Receive Date: 24.12.2024 *Accepted Date: 21.03.2025*

Cost optimization in microgrids: A scenario-based analysis by using polar the fox optimization algorithm

Nisa NACAR ÇIKAN [a*]

[a] *Çukurova University, Department of Electrical and Electronics Engineering, Adana, 01330, Türkiye*
ORCID:0000-0002-9641-4616

Abstract

Microgrids have come up as a promising solution for ensuring efficient, reliable, and sustainable energy management through the distributed energy resources integration. However, some challenges such as integration of distributed generators, economic efficacy and operational constraints cause the management and operation of microgrids remain as a complex problem. In this work, a comprehensive analysis is realized by using the Polar Fox Optimization algorithm to find solutions to these problems. Four different scenarios are analyzed to examine the effects of operational constraints on system performance and economic costs. In the first case, all distributed energy resources are operated within the specified limits and all power from renewable sources is injected into the microgrid. This scenario results in an operating cost of 269.76 €/day. In the second case, the output power of the renewable distributed energy sources is optimized. This case, a cost reduction of 42.5% is obtained when compared to the first scenario. In the third case, the energy exchange constraint between the grid and the microgrid is removed. Thus, a cost reduction of 74.7% is obtained when compared to the first case. In the fourth case, a detailed battery energy storage system model is added by considering technical parameters such as battery efficiency, state-of-charge limits, and charge/discharge rates. This case an operating cost of €107.08/day is obtained. Thus, a cost reduction of 60.3% is obtained when compared to the first case. The results show that changing the operational constraints significantly affects both system performance and economic efficiency. The proposed approach presents valuable perception for microgrid operators and planners. It points out the importance of the optimization algorithm in achieving economically efficient and reliable energy management.

Keywords: Microgrid optimization; Energy management; Renewable integration; Battery storage systems; Grid exchange; Operational constraints

[*] Corresponding author. Tel.: +90-0322-338-6868 Ext: 124
E-mail address: ncikan@cu.edu.tr

1. Introduction

Microgrids (MGs) integrate various distributed energy resources (DERs) to provide reliable, efficient, and sustainable energy solutions. These systems typically consist of distributed generators (DGs) such as photovoltaic (PV) panels, wind turbines (WT), and energy storage systems like batteries, capacitors, and controllable loads [1-3]. These systems offer efficient, reliable, and environmentally friendly solutions for energy management with the integration of renewable DGs [4]. MGs operate in both islanded mode and grid-connected mode unlike traditional centralized power grids. In grid-connected mode, MGs can exchange power with the main grid to optimize energy costs and stability. In islanded mode, they can independently supply power to critical loads during grid outages or in remote areas without grid access [5]. These operations make MGs a key component of modern energy infrastructure in areas with limited grid access. The renewable energy sources (RES) penetration in MGs not only reduces greenhouse gas emissions but also mitigates the dependency on fossil fuels. Furthermore, MGs show a pivotal duty in modern energy infrastructure by supporting the intermittent renewable energy sources integration, improving energy efficiency, and providing backup power during emergencies. For instance, the Santa Rita Jail microgrid in California includes solar PV, fuel cells, and battery storage. Thus, it provides uninterrupted power supply during grid failures and reduces energy costs [6]. Another example is the Bornholm Island microgrid in Denmark. It ensures over 50% of the island's energy demand by wind power and other RES [7]. These examples show the importance of MGs in addressing contemporary energy challenges. It also highlights the need for advanced energy management strategies to optimize the MGs performance.

Previous studies on MGs are mainly focused on energy optimization, control strategies, and economic analysis. Energy optimization techniques aim to minimize operational costs while meeting energy demand. Control strategies focus on maintaining system stability and reliability [8]. Economic analyses evaluate the cost-effectiveness of MGs and their potential for reducing energy expenses [8]. There are many studies in the literature investigating the effective operation of MGs [9-11]. These studies are used different optimization methodologies and considered different cases to find the optimal operating range. Optimization methods are analyzed as deterministic and non-deterministic (metaheuristic) approaches [12,13]. Deterministic methods rely on mathematical models and require a continuous, differentiable objective function along with its gradient information to guide the search process. These methods are efficient for problems where such functions are available, offering fast convergence and high accuracy. However, many real-world engineering and scientific problems involve complex, non-linear, or discontinuous objective functions, making deterministic approaches less applicable. This limitation has led to the development of non-deterministic methods, which do not require gradient information and are better suited for handling complex, multi-modal, and high-dimensional optimization problems [13]. Non-deterministic methods, particularly metaheuristic algorithms, are inspired by natural phenomena and employ probabilistic rules to explore the search space. These algorithms can be further classified into several categories based on their inspiration sources. Evolutionary algorithms imitates the principles of natural selection and evolution. Swarm intelligence algorithms simulate the collective behavior of animal groups. Social-based methods, including Teaching-Learning-Based Optimization (TLBO), model human learning and social interactions, while physics-based methods, such as Simulated Annealing (SA) and Gravitational Search Algorithm (GSA), are inspired by physical laws. Each of these methods has unique and different advantages. For instance, swarm-based algorithms show success in exploration. Evolutionary methods are effective in balancing exploration and exploitation. Thus, the algorithm should be chosen depending on the problem. This is provided comprehensive research on improving the performance and adaptability of metaheuristic algorithms [13].

For an effective energy operation management (EOM) in MGs, different novel algorithms have been implemented in recent years. It is tried to find out which algorithm provides the most effective solution to the applied problem. In [14], different metaheuristic algorithms applied to MGs. The study revealed the increasing need for renewable energy

sources. The study also discussed the problems arising from the intermittent energy supply of DGs and their impact on cost analysis. This review paper also emphasizes the importance of metaheuristic algorithms applied to find optimal solutions for the economic operation of MGs and, in fact, sets the direction for future research. In [15], a cost analysis is performed by solving the sizing problem in MGs using PSO algorithm. In the paper, different PSO-based models are considered to see the effectiveness of the algorithm in cost analysis. The impact of these models on energy management, economic dispatch and unit commitment is analyzed. In [16], the application of a dynamic cost penalty is analyzed by taking into account the cost function in case of any battery degradation in the EOM. PSO algorithm was used in the study and savings of up to 44.50% were achieved. In [17], battery energy storage system (BESS)'s optimal size is determined by taking into account the uncertainties due to market prices, load demand, and DGs, and it is also aimed to minimize the grid cost by reducing it. The study employs the 2m point estimate method for uncertainty modeling and uses Whale Optimization Algorithm and Swine Influenza Model Based Optimization with Quarantine (SIMBO-Q) for cost reduction. The results show that incorporating BESS at an optimal size significantly reduces the MG's operation cost.

Early approaches to MG optimization primarily relied on conventional numerical techniques, including interior-point methods, linear programming, quadratic programming, nonlinear programming, and dynamic programming [18]. These classical methods are effective for finding solutions to optimization problems. These are characterized by continuous variables, and differentiable, low dimensionality, single objectives, or simple constraints. Nevertheless, as MG optimization problems have grown in complexity featuring high dimensionality, large-scale systems, multi-objective requirements, mixed constraints, and multiple control variables. These traditional techniques have proven inadequate or require significant preprocessing to yield results. Moreover, they struggle to address dynamic or robust optimization challenges. In contrast, meta-heuristic methods, which are inspired by social adaptation processes or natural selection, employ a combination of random and local search strategies. Metaheuristic algorithms have been widely applied to various engineering problems, demonstrating their versatility and effectiveness in solving complex optimization tasks [12,13,19-24]. Unlike classical techniques, meta-heuristic approaches are less prone to becoming trapped in local optima, do not rely on specific problem structures or domains, and demonstrate strong adaptability to diverse environments and problem types. They are capable of providing effective solutions in most scenarios [18, 25-26]. Additionally, meta-heuristic methods can dynamically adjust algorithm parameters and encoding precision during the optimization process, making them suitable for solving dynamic optimization problems [18,27]. They also find solutions for discontinuous, non-convex, and multi-objective optimization tasks. As a result, meta-heuristic methods show significant performance in solving complex MG management problems [18, 28-29]. In [30], microgrid contains photovoltaic, wind, and fuel cell generation along with energy storage devices. This method utilizes the 2m point estimate method (PEM) to solve uncertainties by applying self-adaptive gravitational search algorithm (SGSA). The study aims to optimize the operational costs of the microgrid by considering uncertainties in market prices, load demand, and the generated power by DGs. In this work, Polar Fox Optimization (PFO) algorithm is used for the optimal operation of microgrids [31]. A metaheuristic approach is chosen due to its flexibility and ability to handle the non-linear and complex problems. The algorithm shows a balance between exploration and exploitation which is critical for achieving optimal solutions. This research proposes a detailed BESS model. Unlike previous studies, technical parameters such as battery efficiency, state of charge limits, and charging/discharging rates are considered. Furthermore, the study systematically evaluates the impact of different operational constraints and control strategies through four progressive scenarios: (1) a baseline scenario where all distributed generation units are operational, and the full power output from renewable sources (PV and WT) must be injected into the grid; (2) The scenario in which the power generated from DGs is optimally injected into the grid in accordance with the objective function (there is no obligation to supply all the generated energy to the grid); (3) a scenario removing power exchange limitations with the main grid (utility) to evaluate the impact of MG constraints on system economics; and (4) a scenario incorporating detailed battery storage characteristics and constraints into the optimization framework. In summary, this study investigates four different scenarios. In comparison with previous studies (cases 1-3), improvements have been made numerically in terms of cost and reliability. The main contribution of the study is presented in Case 4. By adding a

detailed BESS model, more realistic optimization results have been achieved. The inclusion of BESS constraints in the optimization with a realistic approach has proven its importance for grid operation. The proposed approach not only enhances the economic efficiency of microgrids but also provides a robust solution for managing complex operational constraints, making a significant advancement in the field of microgrid energy management.

Section 2 introduces the problem formulation; section 3 outlines the algorithm used in the paper. In Section 4, simulation results are presented and discussed. Furthermore, 4 different scenarios are presented to show the impact of the PFO algorithm on the cost minimization problem. The last section is the conclusion.

2. Formulation part

The studied MG system consists of multiple DERs and operates in a grid-connected mode at a voltage level of 400V. The primary goal of the MG is to optimize energy dispatch and cost minimization while ensuring reliable power supply to different types of consumers. The parameters are as follows:

- The system includes DGs such as microturbines (MT), PV, fuel cells (FC), and WT.
- A BESS is integrated into the MG to manage load fluctuations and store excess renewable energy.
- The MG can import and export electricity from the utility depending on market prices and operational constraints.

Figure 1 shows the MGs architecture.

In this section, cost is chosen as the objective function. The mathematical formulas are presented for minimization of the total operating cost. The constraints for system reliability and stability are also provided. Additionally, mathematical models for each DG are presented.

2.1. Objective function

The objective function of this study is the minimization of the total operational cost. For this purpose, the generation units and storage systems must be operated optimally within a certain period. The minimum cost function formula is shown in Eq. 1[32].

$$\min_{q}(\text{Cost}) = \min_{q} \sum_{t=1}^{T_{\text{Horizon}}} \text{Cost}(q^t, r^t) = \min_{q} \sum_{t=1}^{T_{\text{Horizon}}} \sum_{i=1}^{N_{DG}} [f_{DG}(P_{Gi}^t) + \lambda_t . P_{\text{Grid}}^t] \quad (1)$$

where p^t is the vector of control variables at time t. It includes the active power outputs of the storage units and generation. This can be written as in Eq. 2.

$$q^t = \left[P_{G1}^t, P_{G2}^t, \dots, P_{GN_G}^t\right] \quad (2)$$

Additionally, r^t denotes the amount of active power exchanged with the utility at time t. It is shown in Eq. 3.

$$r^t = P_{\text{Grid}}^t \quad (3)$$

Here, T_{Horizon} is the time intervals in the optimization period. N_{DG} demonstrated the number of DGs. P_{Gi}^t is active power output of the i-th DG unit at time t. $f_{DG}(P_{Gi}^t)$ is the cost associated with the power generation of the i-th unit. P_{Grid}^t is the power exchanged with the utility at time t. λ_t shows the market price of electricity. The function $f_{DG}(P_{Gi}^t)$ is typically nonlinear, reflecting the complex nature of generation cost functions. The term $\lambda_t . P_{\text{Grid}}^t$ represents the economic cost of purchasing or selling electricity with the utility at time t.

The objective function in Eq. 1 is inherently nonlinear. Specifically, $f_{DG}(P_{Gi}^t)$ shows the complex nature of

generation cost functions. It includes quadratic terms (e.g.,$c(P_{Gi}^{t})^2$) or other nonlinear components. Additionally, the cost associated with power exchange with the grid (λ_t. P_{Grid}^{t}) introduces a piecewise linear component. These nonlinearities are resulted from the complex interactions between generation units, storage systems, and grid exchange.

2.2. Operational constraints

The optimal operation of the microgrid system must satisfy various technical and operational constraints to ensure reliable and stable performance. These constraints include power balance requirements, generation limits of distributed energy resources, energy storage system limitations, and grid power exchange boundaries. The following constraints are considered in the optimization framework for secure and efficient operation of the microgrid.

2.2.1. Micro turbine

The operational constraints of the microturbine are defined by Eq. 4.
Power output limits:

$$P_{MT,min} \leq P_{MT} \leq P_{MT,max} \tag{4}$$

where $P_{MT,min}$ and $P_{MT,max}$ represent the minimum and maximum power outputs respectively. As specified in Table 1, the MT operates within a power range of 6-30 kW with an associated cost coefficient of 0.457 €/kWh. The dynamic operation of MT must respect these power limits while maintaining system stability and meeting demand requirements. These constraints ensure that the MT operates within its technical capabilities while providing reliable power output for microgrid operation.
RD_{MT} and RU_{MT}, is given Eq. 5, represent the ramp-down and ramp-up rates respectively, and t denotes the time interval.

$$-RD_{MT} \leq P_{MT}^{(t)} - P_{MT}^{t-1} \leq RU_{MT} \tag{5}$$

2.2.2. Pem Fuel Cell

Power output limits:

$$P_{FC,min} \leq P_{FC} \leq P_{FC,max} \tag{6}$$

Ramp rate constraints:

$$-RD_{FC} \leq P_{FC}^{t} - P_{FC}^{t-1} \leq RU_{FC} \tag{7}$$

where $P_{FC,min}$ and $P_{FC,max}$ are the minimum and maximum power outputs (3-30 kW in the current study) RD_{FC} and RU_{FC} represent ramp-down and ramp-up rates respectively, as shown in Eq. 6. The dynamic operation of the fuel cell is constrained by its ramp rates as expressed in Eq. 7, where t denotes the time interval.

2.2.3. Energy storage system

The BESS power output is constrained by its rated capacity as shown in Eq. 8, where P_{rated} represents the maximum charging/discharging power capability (±30 kW).
Power limits:

$$-P_{Rated} \leq P_b(t) \leq P_{rated} \quad (8)$$

The state of charge must be maintained within operational limits as defined in Eq. 9, where SoC_{min} and SoC_{max} are set to 20% and 90% respectively to protect battery life and ensure reliable operation. For initialization purposes, the initial state of charge ($SoC_{initial}$) is defined as 50% of the total capacity.
State of charge limits:

$$SoC_{min} \leq SoC(t) \leq SoC_{max} \quad (9)$$

2.2.4. Photovoltaic panels

The power output of the PV system is bounded by the constraints expressed in Eq. 10, where the lower bound represents zero output during periods of no solar irradiance, and $P_{PV,max}$ represents the maximum power output capacity of 25 kW. This constraint ensures that the PV generation remains within its physical limitations while accounting for the intermittent nature of solar resources. Note that the actual power output at any time t depends on the available solar irradiance and ambient temperature conditions but cannot exceed the rated capacity defined in Eq. 10.
Power output limits:

$$0 \leq P_{PV}(t) \leq P_{PV,max} \quad (10)$$

where $P_{PV,max}$ is equal 25 kW (rated capacity) in this study.

2.2.5. Utility

The power exchange between the microgrid and utility grid is subject to constraints as defined in Eq. 11, where $P_{grid,min}$ and $P_{grid,max}$ are set to -30 kW and +30 kW respectively for Case-1 and Case-2. The negative value indicates power export to the utility grid, while positive value represents power import from the utility grid. It should be noted that in Cases 3-4, these power exchange limitations are removed, allowing unrestricted power transactions with the main grid. This constraint plays a crucial role in determining the optimal operation strategy and overall system economics, particularly during periods of high price differentials or significant renewable generation fluctuations.
Power exchange limits for Case-1 and Case-2:

$$-30\,\text{kW} \leq P_{grid}(t) \leq 30\,\text{kW} \quad (11)$$

The limitation specified in Eq.11 is not taken into account in case 3 and case 4. The constraints in the optimization model include both linear and nonlinear components. The power exchange constraint (Eq. 11) is linear, as it defines a simple range for power import/export between the microgrid and the utility grid. However, the battery storage system constraints (Eqs. 8, 9, and 18) introduce nonlinearity due to the inclusion of charging/discharging efficiencies (η_{charge} and $\eta_{discharge}$) and the state of charge dynamics (SoC(t)). These nonlinear constraints significantly affect the overall

structure of the optimization problem, making it more complex and requiring advanced optimization techniques for effective solution.

2.3. DG's model

The MG studied in this study includes DGs such as PV and WT, generators such as MT and FC, and energy storage systems. Each DG unit needs to be properly modeled to operate optimally. In this section, mathematical models of operational characteristics and constraints of DGs are presented.

2.3.1. Micro turbine

Microturbines are tiny gas turbines that can creates both heat and electricity. Their electrical output ranges from about 25-250 kW. The reasons why microturbines are preferred in MGs include their high efficiency and low emission release. The MT consists of a compressor, turbine, combustor, and permanent magnet generator operating at high speeds (typically 50,000-120,000 rpm).

I. Cost function

Eq. 12 shows the operational cost calculation of the MT [33]:

$$C_{MT}(P_{MT}) = a + bP_{MT} + c(P_{MT})^2 \quad (12)$$

where P_{MT} is the output power(kW), C_{MT} is the operational cost (€/h), and a, b, c are the cost coefficients.

II. Fuel cost

The calculation of the fuel cost is demonstrated in Eq.13.

$$C_{fuel} = F \times HR \times P_{MT} \quad (13)$$

where F is the fuel price (€/m³), C_{fuel} is the fuel cost (€/kWh), HR is the heat rate (m³/kWh), and P_{MT} is the power output (kW).

III. Operation & maintenance cost

The costs calculation for maintenance and operation are shown in Eq.14.

$$C_{O\&M} = K_{O\&M} \times P_{MT} \quad (14)$$

where $K_{O\&M}$ is the O&M coefficient (€/kWh) and $C_{O\&M}$ is the O&M cost (€/kWh).

IV. Start-up/Shut-down Cost

Eq. 15 shows the cost calculation for Start-up/shut-down.

$$\frac{C_{SU}}{SD} = \frac{K_{SU}}{SD} \times \frac{N_{SU}}{SD} \quad (15)$$

where the $\frac{N_{SU}}{SD}$ is the number of start-ups/shut-downs events and the $\frac{K_{SU}}{SD}$ is the start-up/shut-down cost coefficient.

V. Total bid calculation:

Eq. 16 shows the total bid calculation.

$$\mathrm{Bid_{MT}} = (\mathrm{C_{fuel}} + \mathrm{C_{O\&M}}) \times (1 + \mathrm{P_{margin}}) \quad (16)$$

Here, $\mathrm{P_{margin}}$ is the profit margin (typically taken as 10-20%).

In order to optimally price MTs, analysis of many components is required. The main one among these components is the fuel cost. This cost is calculated by multiplication of the heat rate, fuel price and power output of the MT unit. The production of the heat rate (m^3/kWh), fuel price(€/m^3), and the MT power output (kW) give the fuel cost in terms of €/h. Another component is the operation and maintenance (O&M) cost, which takes into account component wear, routine maintenance, and so on. Shutdown and start-up costs are important, especially in high-cycle operations. Especially in frequent cycle operations, the closing and start-up costs are important. The cost here is obtained by multiplying the closing/start-up coefficients by the number of cycles. In the final price offer, all costs are added and formulated by adding a profit margin, usually between 10% and 20%.

In this study, considering the local market conditions and the operational characteristics of the MT system and taking all costs into account, it was determined as 0.457 €/kWh.

2.3.2. Pem fuel cell

Proton exchange membrane fuel cells (PEM FC) directly and efficiently convert chemical energy stored in fuel into electrical energy. In MG applications, PEMFCs offer several advantages including high efficiency, quick start-up capability, and environmental benefits due to zero emissions during operation. PEMFCs typically operate at low temperatures (60-80°C) which makes them suitable for power generation applications.

The cost of the PEM FCs can be calculated as in Eq. 17.

$$\mathrm{C_{FC}}(\mathrm{P_{FC}}) = \alpha_{\mathrm{FC}} + \beta_{\mathrm{FC}} \times \mathrm{P_{FC}} + \gamma_{\mathrm{FC}} \times (\mathrm{P_{FC}})^2 \quad (17)$$

Here, $\mathrm{P_{FC}}$ is the power output (kW), $\mathrm{C_{FC}}$is the operational cost (€/h), α_{FC}, β_{FC}, γ_{FC} are the cost coefficients.

In this work, the cost of PEMFC is determined as 0.294 €/kWh. This price is lower than the MT price, indicating that PEMFCs operate at high efficiency and low operating costs. This cost advantage makes PEMFC an economically attractive option for MG operations, particularly during periods of high energy demand or when renewable sources are unavailable.

2.3.3. Energy storage systems

The BESS plays an important role in MG operation by providing power balance, peak shaving capabilities, and economic optimization through energy arbitrage. In this study, a NiMH battery system is implemented with a rated power capacity of 30 kW and energy capacity of 400 kWh, enabling efficient energy management and grid support functionalities.

I. Mathematical model:

The state of charge (SoC) dynamics can be expressed as [34]:

$$\mathrm{SoC(t)} = \mathrm{SoC(t-1)} + \left(\eta_{\mathrm{charge}}.\mathrm{P_{charge}(t)} - \frac{\mathrm{P_{discharge}(t)}}{\eta_{\mathrm{discharge}}}\right)\left(\frac{\Delta \mathrm{t}}{\mathrm{C_b}}\right) \quad (18)$$

where SoC(t) is the state of charge at time t, η_{charge} and $\eta_{\mathrm{discharge}}$ are charging and discharging efficiencies (95% and 92% respectively). $\mathrm{P_{charge}(t)}$ and $\mathrm{P_{discharge}(t)}$ represent charging and discharging power, $C_b$is the battery capacity (400 kWh), and $\Delta \mathrm{t}$ is the time interval.

II. Cost function:

The operational cost of BESS is shown in Eq. 19.

$$C_{BESS} = C_{deg} \times |P_b(t)| + C_{O\&M} \quad (19)$$

Here, $C_{O\&M}$ is operation and maintenance cost and C_{deg} indicates the degradation cost. The total bid cost is set at 0.38 €/kWh. Here, the total cost is determined as 0.38 €/kWh. BESS works bidirectionally, allowing both injection and absorption of power. Thus, it responds more flexibly to the changing load demands of the MG and the changing price signals accordingly.

2.3.4. Photovoltaic panels

PVs are an important renewal DG in MGs. They convert solar radiation directly into electrical energy through semiconductor materials. The power output produced depends entirely on solar radiation. In this work, the PV system has a rated capacity of 25 kW, with its actual power output varying throughout the day based on solar radiation intensity.

I. Mathematical model:

The PV output power can be calculated as in Eq. 20.

$$P_{PV}(t) = \eta_{PV} \times A \times G(t) \times \left(1 - \beta(T_c(t) - T_{ref})\right) \quad (20)$$

where η_{PV} is the overall system efficiency, A is the total area of PV panels (m²), G(t) is the solar irradiance (kW/m²), β is the temperature coefficient (%/°C), $T_c(t)$ is the cell temperature, and T_{ref} is the reference temperature (25°C)

II. The generation cost structure includes:

$$C_{PV} = \frac{C_{capital}}{N} + C_{O\&M} \quad (21)$$

where $C_{capital}$ is the annualized capital cost, N is the number of operational hours per year, $C_{O\&M}$ represents operation and maintenance costs. The total bid cost is set at 2.584 €/kWh.

The PV system's output exhibits daily and seasonal variations, with peak generation occurring around 13:00 hours in the current study, reaching approximately 23.9 kW. Despite having no fuel costs, the relatively high bid price reflects the capital investment and maintenance requirements. The system's intermittent nature necessitates coordination with other microgrid components, particularly the battery storage system and conventional generators, to ensure reliable power supply. The optimization algorithm considers both mandatory full power injection (Case-1) and flexible power injection (Cases 2-4) scenarios, allowing for comprehensive evaluation of different operational strategies while maintaining system stability and economic efficiency.

2.3.5. Utility

The microgrid maintains continuous power exchange with the main grid (utility), enabling both power import during high demand or low local generation periods and power export during excess generation. The bidirectional power flow is governed by economic and technical constraints.

Given the nonlinearity of the objective function and the presence of nonlinear constraints, the proposed optimization problem is classified as a nonlinear optimization model. Although the problem is solved using a metaheuristic algorithm (Polar Fox Optimization), the mathematical structure of the problem remains nonlinear due to the quadratic cost terms of distributed generation units and the efficiency-based constraints of the battery storage system. This classification is essential for understanding the complexity of the problem and the need for advanced optimization techniques to achieve an effective solution.

I. Mathematical model:

The power exchange with utility can be expressed as [1,35]:

$$P_{grid}(t) = P_{load}(t) - [P_{MT}(t) + P_{FC}(t) + P_{PV}(t) + P_{WT}(t) \pm P_{BAT}(t)] \quad (22)$$

where $P_{grid}(t) > 0$ represents power import from utility, $P_{grid}(t) < 0$ represents power export to utility.

II. Cost/Revenue Function:

$$C_{grid}(t) = P_{grid}(t) \times B_{grid}(t) \quad (23)$$

Here, $C_{grid}(t) > 0$ denotes the cost (import), $B_{grid}(t)$ is the time-varying utility bid price, and $C_{grid}(t) < 0$ indicates the revenue (export).

Utility bid cost varies according to the peak hours of the day. For example, it is 0.12 €/kWh in the early morning hours, while it becomes 4.00 €/kWh during the peak hours, which include the 10:00-14:00 period. The change here once again shows the importance and necessity of the optimization study. During peak hours, it maximizes power export by using all the DERs available in the MG. During low-price periods, it imports power for consumption and battery charging. Thus, this bidirectional change is important in cost function optimization studies.

3. Polar fox optimization algorithm

PFO is a metaheuristic algorithm inspired by hunting behaviours and movements of arctic foxes [31]. In the PFO algorithm, a group of "arctic foxes" explore a solution space to find the global optimum of the objective function. The location of each fox is represented as a vector in the solution space, represented as $X_i = [x_{i1}, x_{i2}, \dots, x_{id}]$, where i refers to the fox index and d represents the dimension of the problem. The PFO algorithm uses two main strategies for movement: global exploration (random movement) and local exploitation (interactions between individuals). The algorithm employs two main strategies for movement: a global exploration strategy (simulating random movement) and a local exploitation strategy (based on interactions between individuals). Mathematically, the position of each fox is updated iteratively using the Eq. 24.

$$X_i^{new} = X_i^{old} + \alpha.(X_{best} - X_i) + \beta.(X_{rand} - X_i) \quad (24)$$

where, X_{best} is the best-known solution (global best), X_{rand} is a randomly selected fox, α and β are scaling factors that control the exploration and exploitation behaviors, X_i^{new} and X_i^{old} are the updated and previous positions of the fox, respectively. These movements allow the foxes to converge towards the optimal solution, balancing exploration, and exploitation throughout the search process. The PFO algorithm has been shown to effectively solve complex and nonlinear problems, outperforming many traditional optimization methods in terms of both accuracy and convergence speed.

4. Simulation results

The structure of the proposed system for optimal operation of microgrids is shown in Figure 1. The test system is a typical low-voltage microgrid containing DGs including a fuel cell (FC), micro-turbine (MT), WT, and PV. Additionally, the system includes a battery as an energy storage unit. The microgrid operates in grid-connected mode at 400V level and serves three different load zones (industrial, commercial, and residential). The technical specifications and cost data of the generation units in the system are presented in Tables 1 and 2. The minimum-maximum generation capacities and operating costs (€/kWh) of each unit are specified. The battery system has a ±30 kW power capacity and can perform charging/discharging operations. Power exchange with the main grid is also limited to ±30 kW. Figure 2 shows the load demand, PV and WT generation, and grid price variations during the 24-hour operation period of the system. The load demand varies between 50-90 kW throughout the day. While PV generation reaches its peak value of approximately 24 kW at 13:00 due to maximum solar radiation intensity, WT generation shows variability depending on wind speed. Grid electricity prices remain particularly high during peak hours (between 9:00-16:00). In light of this data, minimum-cost generation planning has been performed for optimal MG operation under different scenarios. The operation strategy has been developed considering the technical constraints of all units and system reliability. The suggested approach aims to minimize the total operating cost while maintaining power balance and satisfying various operational constraints such as generation limits, battery storage characteristics, and grid exchange limitations.

The mathematical formulation and detailed analysis of different operational scenarios will be presented in the following sections to show the proposed optimization technique's effectiveness in achieving economical and reliable microgrid operation. In this study, four different operational scenarios are investigated to analyse the optimal operation management of the microgrid system:

- Case-1 represents the baseline scenario where all distributed generation units are operational, and the full power output from renewable sources (PV and WT) must be injected into the grid. This case serves as a reference point for comparing other operational strategies.
- Case-2 maintains the same system configuration as Case-1 but introduces flexibility in renewable power integration. Instead of mandatory full power injection, PV and WT outputs are treated as optimization variables, allowing the system to determine the optimal level of renewable power utilization.
- Case-3 extends Case-2 by removing the power exchange limitations with the main grid. While Case-1 and Case-2 operate under strict grid power exchange constraints (±30 kW), this case allows unrestricted power exchange to evaluate the impact of grid constraints on system economics.
- Case-4 builds upon Case-3 by incorporating detailed battery storage characteristics into the optimization framework. This scenario considers technical parameters such as battery efficiency, state of charge limits, and charging/discharging rates to provide a more realistic assessment of storage system integration.

Through these progressive scenarios, it is aimed to systematically evaluate the impact of different operational constraints and control strategies on microgrid performance and economic efficiency. This framework helps identify the most effective operational strategy considering various technical and economic factors affecting microgrid operation.

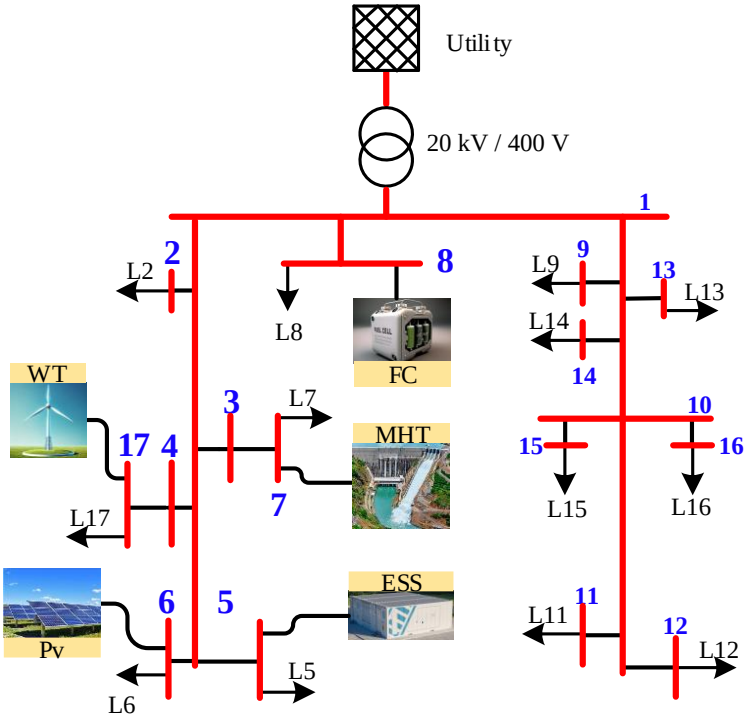

Fig. 1. Single-line diagram of the proposed low-voltage microgrid with distributed generation units [36]

Table 1. Power output limitations and cost parameters of generation units [1]

ID	Generator Type	Min Power Generation [kW]	Max Power Generation [kW]	Bid (€/kWh)
1	Battery	-30	30	0.380
2	PEM FC	3.0	30	0.294
3	PV	0.0	25	2.584
4	WT	0.0	15	1.073
5	MT	6.0	30	0.457
6	Utility	-30	30	In Table (2) Column (5)

Table 2. Technical specifications of distributed generation units in the microgrid [1,35,36]

Hour	Photovoltaic [kW]	Wind Turbine [kW]	Load [kW]	Utility (€/kWh)
1	0.0000	1.7850	52.000	0.2300
2	0.0000	1.7850	50.000	0.1900
3	0.0000	1.7850	50.000	0.1400

4	0.0000	1.7850	51.000	0.1200
5	0.0000	1.7850	56.000	0.1200
6	0.0000	0.9150	63.000	0.2000
7	0.0000	1.7850	70.000	0.2300
8	0.2000	1.3050	75.000	0.3800
9	3.7500	1.7850	76.000	1.5000
10	7.5250	3.0900	80.000	4.0000
11	10.4500	8.7750	78.000	4.0000
12	11.9500	10.4100	74.000	4.0000
13	23.9000	3.9150	72.000	1.5000
14	21.0500	2.3700	72.000	4.0000
15	7.8750	1.7850	76.000	2.0000
16	4.2250	1.3050	80.000	1.9500
17	0.5500	1.7850	85.000	0.6000
18	0.0000	1.7850	88.000	0.4100
19	0.0000	1.3020	90.000	0.3500
20	0.0000	1.7850	87.000	0.4300
21	0.0000	1.3005	78.000	1.1700
22	0.0000	1.3005	71.000	0.5400
23	0.0000	0.9150	65.000	0.3000
24	0.0000	0.6150	56.000	0.2600

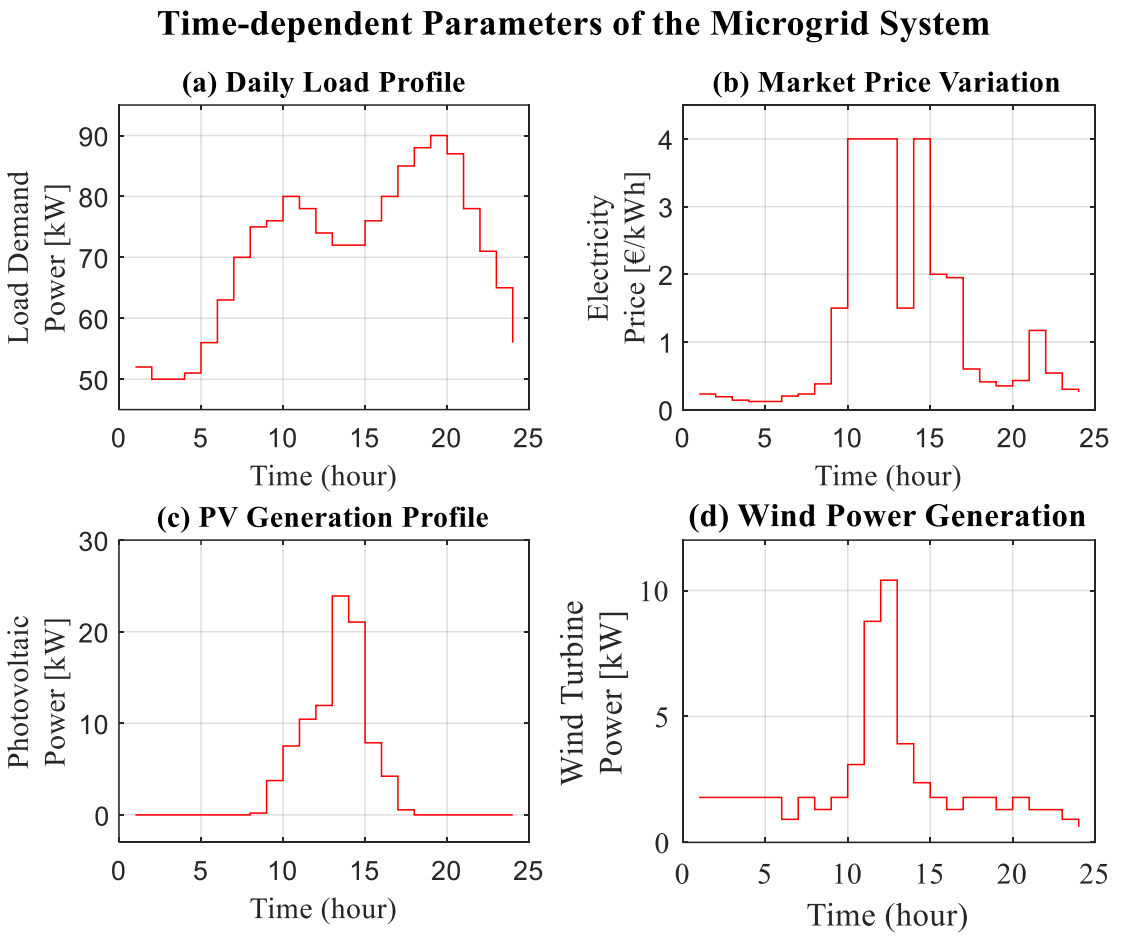

Fig. 2. Time-dependent parameters of the microgrid over 24 hours: (a) Load demand, (b) Grid electricity prices (c) PV power availability and, (d) WT power availability.

4.1. Case-1: system operation under complete renewable power injection

The performance analysis of Case-1, where all DG units are operational and full power from PV and WT is injected into the grid, is presented in Table 3 and Figure 3. The results demonstrate several key operational characteristics over the 24-hour period, revealing distinct patterns in different time intervals.

During early morning hours (00:00-06:00), the system operates under low grid prices ranging from 0.12 to 0.23 €/kWh. In this period, the battery system operates in charging mode, storing energy between -11.7 to -17.7 kW. Simultaneously, both MT and FC maintain their minimum output levels of 6 kW and 30 kW respectively, responding to the combination of low demand and prices.

The operational strategy undergoes a significant shift during peak hours (09:00-14:00) when grid prices surge to 4.0 €/kWh. During these hours, the MT outputs maximum capacity, while the battery goes into maximum discharge mode. MG efficiently exports excess power to the grid and reaches up to -30 kW. This shows that the stored energy is used efficiently during peak hours. Renewable DGs contribute at different rates throughout the day. For example, PV generation reaches its maximum level at 23.9 kW around 13:00, while WT produces between 0.61-10.41 kW. By

applying the PFO algorithm to the optimization problem, the system is operated stably. During the evening hours (17:00-21:00), the power demand in the system increases. However, during the same hours, there is a decrease in the power production of renewable DGs. Therefore, the grid is supported by the power provided by MT, FC and battery during the evening hours.

The total operating cost for Case-1 is calculated as 269.76 €/day. This baseline scenario effectively demonstrates system operation under full renewable power injection constraints, showcasing successful coordination between dispatchable units (MT, FC), storage system, and grid exchanges while minimizing operational costs and meeting demand requirements. The effectiveness of this operational strategy can be further evaluated through comparison with subsequent cases to assess potential improvements in operational efficiency and cost reduction.

Table 3. Hourly optimal dispatch results and operational costs for Case-1 with full renewable power integration

Time Hour	Fuel Cell [kW]	Micro Turbine [kW]	Wind Turbine [kW]	PV [kW]	Utility (€/kWh)	Cost (€/kWh)	Energy Storage [kW]
1	30.0000	6.0000	1.7850	0.0000	30.0000	14.3790	-15.7850
2	30.0000	6.0000	1.7850	0.0000	30.0000	12.4190	-17.7850
3	30.0000	6.0000	1.7850	0.0000	30.0000	10.9190	-17.7850
4	30.0000	6.0000	1.7850	0.0000	30.0000	10.6990	-16.7850
5	30.0000	6.0000	1.7850	0.0000	30.0000	12.5990	-11.7850
6	30.0000	6.0000	0.9150	0.0000	30.0000	17.0561	-3.9150
7	30.0000	6.0000	1.7850	0.0000	30.0000	21.2190	2.2150
8	30.0000	6.0000	1.3050	0.2000	10.3031	27.7272	27.1919
9	30.0000	30.0000	1.7850	3.7500	-19.5350	16.2328	30.0000
10	30.0000	30.0000	3.0900	7.5250	-20.6150	-25.7698	30.0000
11	30.0000	28.7750	8.7750	10.4500	-30.0000	-50.2115	30.0000
12	30.0000	21.6400	10.4100	11.9500	-30.0000	-47.8418	30.0000
13	30.0000	14.1850	3.9150	23.9000	-30.0000	47.6609	30.0000
14	30.0000	18.5800	2.3700	21.0500	-30.0000	-34.3527	30.0000
15	30.0000	30.0000	1.7850	7.8750	-23.6600	8.8743	30.0000
16	30.0000	30.0000	1.3050	4.2250	-15.5300	15.9642	30.0000
17	30.0000	30.0000	1.7850	0.5500	-7.3350	32.8655	30.0000
18	30.0000	6.0000	1.7850	0.0000	20.2150	33.1655	30.0000
19	30.0000	6.0000	1.3020	0.0000	30.0000	32.0843	22.6980
20	30.0000	6.0000	1.7850	0.0000	19.2150	33.1398	30.0000
21	30.0000	30.0000	1.3005	0.0000	-13.3005	19.7639	30.0000
22	30.0000	30.0000	1.3005	0.0000	-20.3005	24.3632	30.0000
23	30.0000	6.0000	0.9150	0.0000	30.0000	20.8161	-1.9150
24	30.0000	6.0000	0.6150	0.0000	30.0000	15.9882	-10.6150
---	---	---	---	---	**Total Cost:**	**269.7599**	---

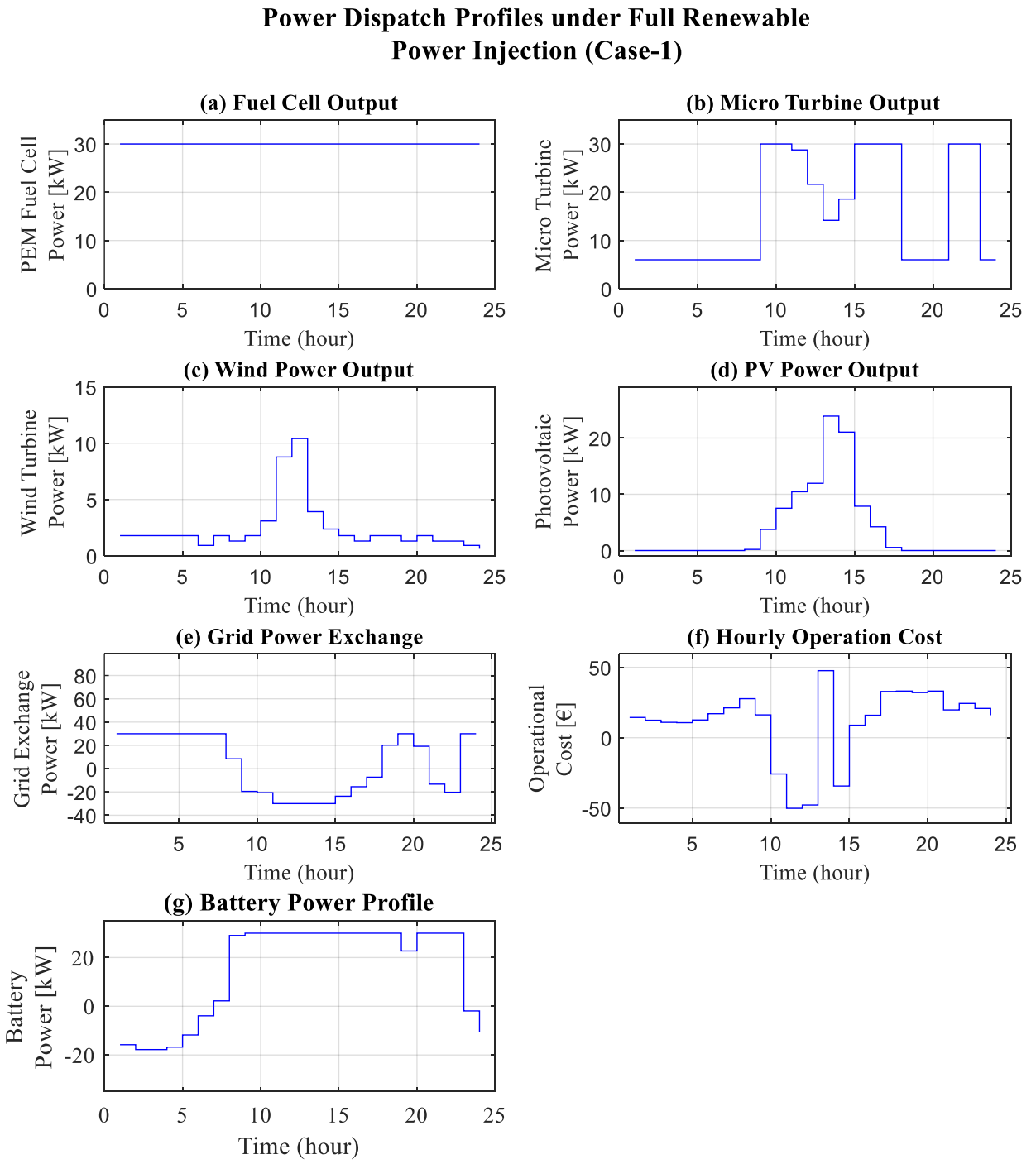

Fig. 3. Power dispatch profiles and system performance under full renewable injection (Case-1: Generation unit outputs a-FC, b-MT, c-WT, d-PV, e-Grid exchange power, f-Hourly operational cost, and g-Battery power.)

4.2. Case-2: operational optimization with controllable renewable integration

In this study, Case-2 examines the operational optimization where renewable power (PV and WT) injection is considered as a decision variable, unlike Case-1 where complete injection of renewable generation was mandatory. The optimization results, presented in Table 4 and Figure 4, reveal several significant findings.

The total operational cost decreased to 155.01 €/day, representing a substantial 42.5% reduction compared to Case-1 (269.76 €/day). This remarkable improvement demonstrates the advantages of flexible renewable power integration. During low-price periods (00:00-07:00), the optimization strategy-maintained MT and FC at their minimum outputs (6 kW and 30 kW respectively) while completely curtailing PV and WT generation. Throughout this period, the battery operated in charging mode with values ranging from -3 to -16 kW, storing energy for high-price periods.

During peak price hours (09:00-14:00), the system implemented various strategies to maximize economic benefits. These strategies included operating MT and FC at full capacity (30 kW each), selectively utilizing renewable generation (e.g., 7.52 kW from PV and 3.09 kW from WT at 10:00), maintaining battery discharge at maximum capacity (30 kW), and exporting power to the grid when profitable.

In the evening period (17:00-22:00), the system coordinated battery discharge and conventional generation (MT, FC) in a balanced manner to minimize grid power import during moderate price periods. This case study demonstrates that optimal scheduling of renewable power injection can significantly enhance economic performance while maintaining system stability and meeting demand requirements. The results clearly indicate that allowing flexibility in renewable power integration can lead to more cost-effective operation of the microgrid system.

Table 4. Optimal dispatch results for Case-2: flexible renewable power integration strategy

Time Hour	Fuel Cell [kW]	Micro Turbine [kW]	Wind Turbine [kW]	PV [kW]	Utility (€/kWh)	Cost (€/kWh)	Energy Storage [kW]
1	30.0000	6.0000	0.0000	0.0000	30.0000	13.1420	-14.0000
2	30.0000	6.0000	0.0000	0.0000	30.0000	11.1820	-16.0000
3	30.0000	6.0000	0.0000	0.0000	30.0000	9.6820	-16.0000
4	30.0000	6.0000	0.0000	0.0000	30.0000	9.4620	-15.0000
5	30.0000	6.0000	0.0000	0.0000	30.0000	11.3620	-10.0000
6	30.0000	6.0000	0.0000	0.0000	30.0000	16.4220	-3.0000
7	30.0000	6.0000	0.0000	0.0000	30.0000	19.9820	4.0000
8	30.0000	6.0000	0.0000	0.0000	9.3328	26.3820	29.6672
9	30.0000	30.0000	1.7850	0.0500	-15.7850	12.1678	30.0000
10	30.0000	30.0000	3.0900	7.5250	-20.6150	-25.7698	30.0000
11	30.0000	30.0000	8.7750	9.2250	-30.0000	-52.8170	30.0000
12	30.0000	30.0000	10.4100	3.5900	-30.0000	-65.6235	30.0000
13	30.0000	30.0000	3.9150	0.0000	-21.9150	5.2583	30.0000
14	30.0000	30.0000	2.3700	9.6300	-30.0000	-58.6431	30.0000
15	30.0000	30.0000	1.7850	7.8750	-15.7850	4.2753	30.0000
16	30.0000	30.0000	1.3050	4.2250	-11.3050	13.2855	30.0000
17	30.0000	30.0000	0.0000	0.5500	-5.0000	30.9300	30.0000
18	30.0000	6.0000	0.0000	0.0000	22.0000	31.9820	30.0000
19	30.0000	6.0000	0.0000	0.0000	30.0000	31.1820	24.0000
20	30.0000	6.0000	0.0000	0.0000	21.0000	31.9920	30.0000

21	30.0000	30.0000	1.3005	0.0000	-13.3005	19.7639	30.0000
22	30.0000	30.0000	0.0000	0.0000	-19.0000	23.6700	30.0000
23	30.0000	6.0000	0.0000	0.0000	30.0000	20.1820	-1.0000
24	30.0000	6.0000	0.0000	0.0000	30.0000	15.5620	-10.0000
---	---	---	---	---	**Total Cost:**	**155.0133**	---

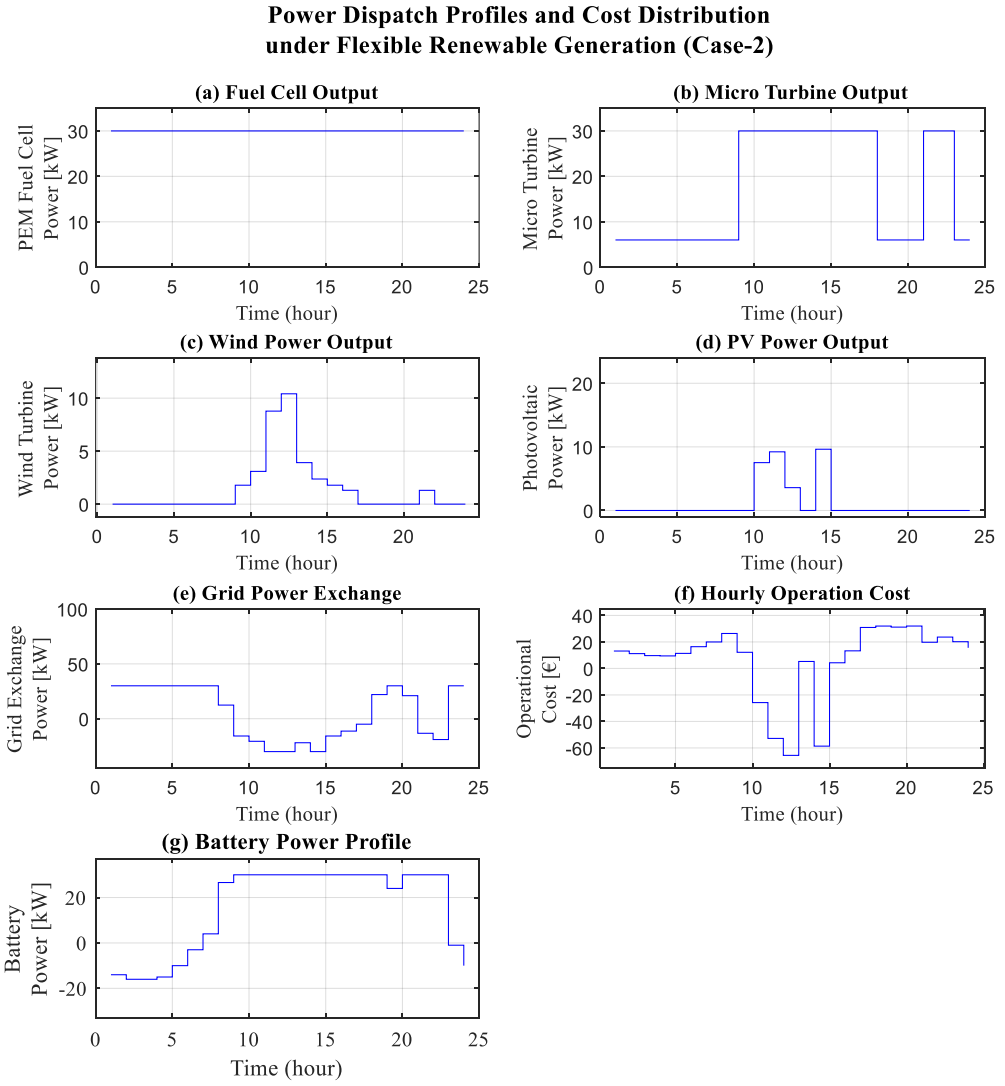

Fig. 4. Optimal power dispatch profiles and cost distribution under flexible renewable generation control (Case-2: Generation unit outputs a-FC, b-MT, c-WT, d-PV, e-Grid exchange power, f-Hourly operational cost, and g-Battery power.)

4.3. Case-3: unrestricted grid exchange with flexible renewable integration

This study examines the impact of removing grid power exchange limitations while maintaining flexible renewable

power integration. The results, presented in Table 5 and Figure 5, demonstrate significant improvements in system economics and operational flexibility. The total operational cost decreased to 68.18 €/day, representing a substantial reduction of 74.7% and 56.0% compared to Case-1 (269.76 €/day) and Case-2 (155.01 €/day), respectively. This remarkable cost reduction highlights the significant economic impact of grid exchange constraints on microgrid operation. During low-price periods (00:00-07:00), the optimization strategy exhibited distinct characteristics. The MT and FC operated at minimum outputs (6 kW and 3 kW respectively), while renewable generation was completely curtailed. The battery maintained maximum charging rate (-30 kW), and significant power import from the grid (up to 91 kW) was utilized to meet demand when prices were low. The peak price period (09:00-14:00) demonstrated aggressive economic optimization through several strategies. These included maximum utilization of all DG units, strategic deployment of renewable resources (e.g., 11.95 kW from PV and 10.41 kW from WT at 12:00), battery discharging at maximum capacity (30 kW), and substantial power export to grid (up to -41.42 kW at 14:00) to capitalize on high prices. Evening operations (17:00-24:00) revealed dynamic switching between import and export modes based on price signals, with grid exchange power varying from -19 kW to 84 kW, demonstrating the benefits of unrestricted grid interaction. The results clearly indicate that removing grid exchange limitations enables more aggressive economic optimization, although practical implementation would require careful consideration of grid stability and infrastructure capabilities. This case effectively illustrates how grid exchange constraints significantly impact the economic efficiency of microgrid operations, where the ability to freely exchange power with the main grid enables the system to better capitalize on price differentials and optimize resource utilization.

Table 5. Optimization results for Case-3: unrestricted grid exchange with flexible renewable integration

Time	Fuel Cell	Micro Turbine	Wind Turbine	PV	Utility	Cost	Energy Storage
Hour	[kW]	[kW]	[kW]	[kW]	(€/kWh)	(€/kWh)	[kW]
1	3.0000	6.0000	0.0000	0.0000	73.0000	9.0140	-30.0000
2	3.0000	6.0000	0.0000	0.0000	71.0000	5.7140	-30.0000
3	3.0000	6.0000	0.0000	0.0000	71.0000	2.1640	-30.0000
4	3.0000	6.0000	0.0000	0.0000	72.0000	0.8640	-30.0000
5	3.0000	6.0000	0.0000	0.0000	77.0000	1.4640	-30.0000
6	3.0000	6.0000	0.0000	0.0000	84.0000	9.0240	-30.0000
7	3.0000	6.0000	0.0000	0.0000	91.0000	13.1540	-30.0000
8	30.0000	6.0000	0.0000	0.0000	22.6887	26.3820	16.3113
9	30.0000	30.0000	1.7850	0.0000	-15.7850	12.1678	30.0000
10	30.0000	30.0000	3.0900	7.5250	-20.6150	-25.7698	30.0000
11	30.0000	30.0000	8.7750	10.4500	-31.2250	-54.5516	30.0000
12	30.0000	30.0000	10.4100	11.9500	-38.3600	-77.4613	30.0000
13	30.0000	30.0000	3.9150	0.0000	-21.9150	5.2583	30.0000
14	30.0000	30.0000	2.3700	21.0500	-41.4200	-74.8138	30.0000
15	30.0000	30.0000	1.7850	0.0000	-15.7850	4.2753	30.0000
16	30.0000	30.0000	1.3050	0.0000	-11.3050	13.2855	30.0000
17	30.0000	30.0000	0.0000	0.0000	-5.0000	30.9300	30.0000
18	30.0000	6.0000	0.0000	0.0000	22.0000	31.9820	30.0000
19	30.0000	6.0000	0.0000	0.0000	84.0000	29.5620	-30.0000
20	30.0000	6.0000	0.0000	0.0000	21.0000	31.9920	30.0000
21	30.0000	30.0000	1.3005	0.0000	-13.3005	19.7639	30.0000

22	30.0000	30.0000	0.0000	0.0000	-19.0000	23.6700	30.0000
23	30.0000	6.0000	0.0000	0.0000	59.0000	17.8620	-30.0000
24	3.0000	6.0000	0.0000	0.0000	77.0000	12.2440	-30.0000
---	---	---	---	---	**Total Cost:**	**68.17626**	---

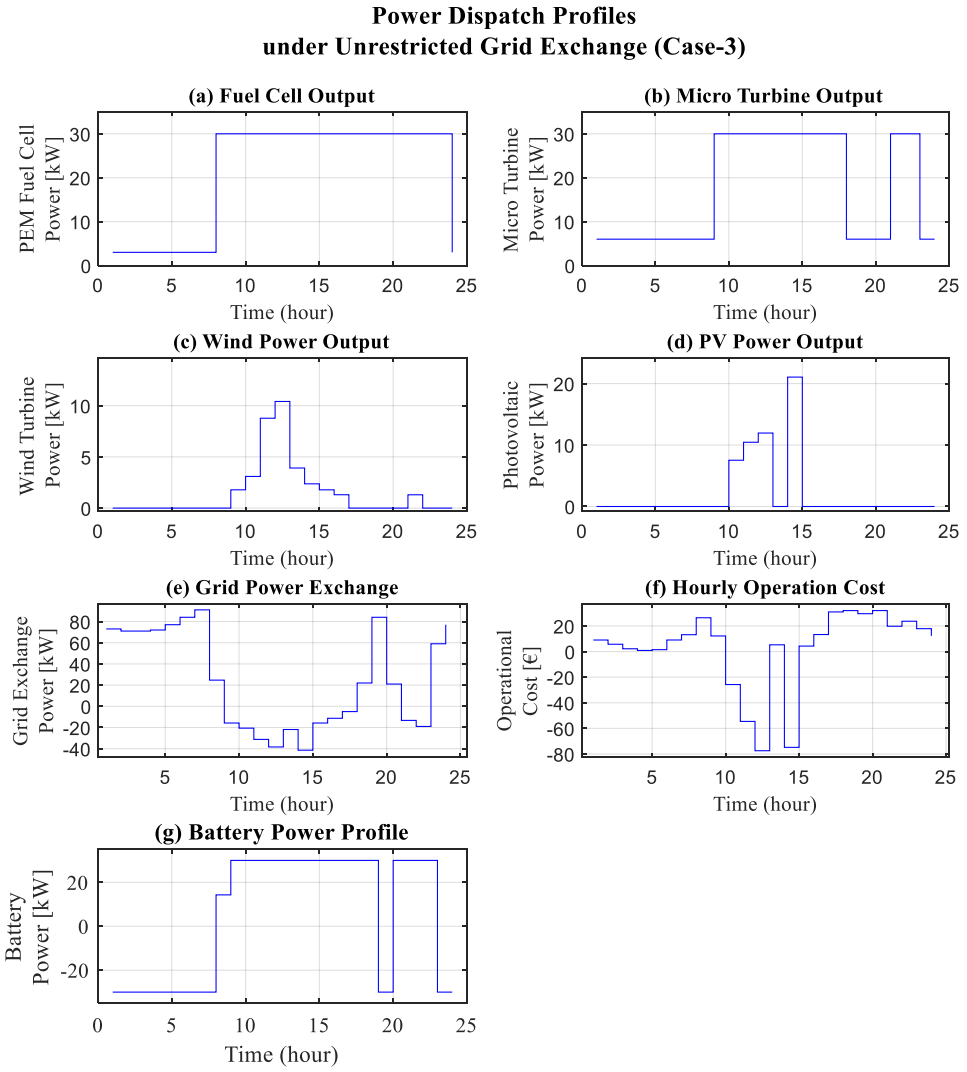

Fig. 5. Power dispatch profiles and economic performance under unrestricted grid exchange conditions (Case-3: Generation unit outputs a-FC, b-MT, c-WT, d-PV, e-Grid exchange power, f-Hourly operational cost, and g-Battery power.)

4.4. Case-4: analysis of microgrid operation with detailed battery energy storage system model

This case study incorporates a detailed BESS model to achieve more realistic optimization results. The BESS is

characterized using Equations 8, 9, and 18. The implementation of detailed battery constraints while maintaining unrestricted grid exchange reveals several significant operational characteristics.

The optimization results demonstrate that the total operational cost amounts to 107.08 €/day. Although this cost is higher than Case-3 (68.18 €/day), it represents a more realistic operational scenario and still achieves substantial cost reductions compared to Cases 1 and 2. This cost differential primarily stems from the incorporation of practical battery constraints, including efficiency losses and state of charge limitations. Analysis of the early morning period (00:00-05:00) demonstrates an optimization strategy focused on leveraging low electricity prices. During these hours, the battery system operates at maximum charging capacity (-30 kW), while distributed generation units maintain minimal output levels with MT and FC operating at 6 kW and 3 kW respectively. This period is characterized by significant grid power imports, serving both the load demand and battery charging requirements efficiently. The system behaviour during peak price periods (09:00-14:00) exhibits sophisticated optimization characteristics. The distributed generation units operate at full capacity, with both MT and FC delivering their maximum output of 30 kW. Renewable power sources are strategically deployed based on availability and economic considerations. Battery discharge operations are carefully optimized while respecting efficiency parameters and SoC constraints, complementing the system's ability to export power to the grid during high-price intervals.

Table 6. Optimal dispatch results for Case-4: integration of detailed battery storage constraints with unrestricted grid exchange

Time	Fuel Cell	Micro Turbine	Wind Turbine	PV	Utility	Cost	Energy Storage
Hour	[kW]	[kW]	[kW]	[kW]	(€/kWh)	(€/kWh)	[kW]
1	3.0000	6.0000	0.0000	0.0000	73.0000	9.0140	-30.0000
2	3.0000	6.0000	0.0000	0.0000	71.0000	5.7140	-30.0000
3	3.0000	6.0000	0.0000	0.0000	71.0000	2.1640	-30.0000
4	3.0000	6.0000	0.0000	0.0000	72.0000	0.8640	-30.0000
5	3.0000	6.0000	0.0000	0.0000	77.0000	1.4640	-30.0000
6	3.0000	6.0000	0.0000	0.0000	72.4211	11.1082	-18.4211
7	3.0000	6.0000	0.0000	0.0000	61.0000	17.6540	-0.0000
8	30.0000	6.0000	0.0000	0.0000	39.0000	26.3820	-0.0000
9	30.0000	30.0000	1.7850	0.0000	-15.7850	12.1678	30.0000
10	30.0000	30.0000	3.0900	7.5250	-20.6150	-25.7698	30.0000
11	30.0000	30.0000	8.7750	10.4500	-31.2250	-54.5516	30.0000
12	30.0000	30.0000	10.4100	11.9500	-38.3600	-77.4613	30.0000
13	30.0000	30.0000	3.9150	0.0000	-21.9150	5.2583	30.0000
14	30.0000	30.0000	2.3700	21.0500	-41.4200	-74.8138	30.0000
15	30.0000	30.0000	1.7850	0.0000	-15.7850	4.2753	30.0000
16	30.0000	30.0000	1.3050	0.0000	-11.3050	13.2855	30.0000
17	30.0000	30.0000	0.0000	0.0000	7.4000	33.6580	17.6000
18	30.0000	6.0000	0.0000	0.0000	52.0000	32.8820	-0.0000
19	30.0000	6.0000	0.0000	0.0000	84.0000	29.5620	-30.0000
20	30.0000	6.0000	0.0000	0.0000	24.7800	32.1810	26.2200
21	30.0000	30.0000	1.3005	0.0000	16.6995	43.4639	0.0000
22	30.0000	30.0000	0.0000	0.0000	11.0000	28.4700	0.0000
23	30.0000	6.0000	0.0000	0.0000	59.0000	17.8620	-30.0000

24	3.0000	6.0000	0.0000	0.0000	77.0000	12.2440	-30.0000
---	---	---	---	---	**Total Cost:**	**107.07747**	---

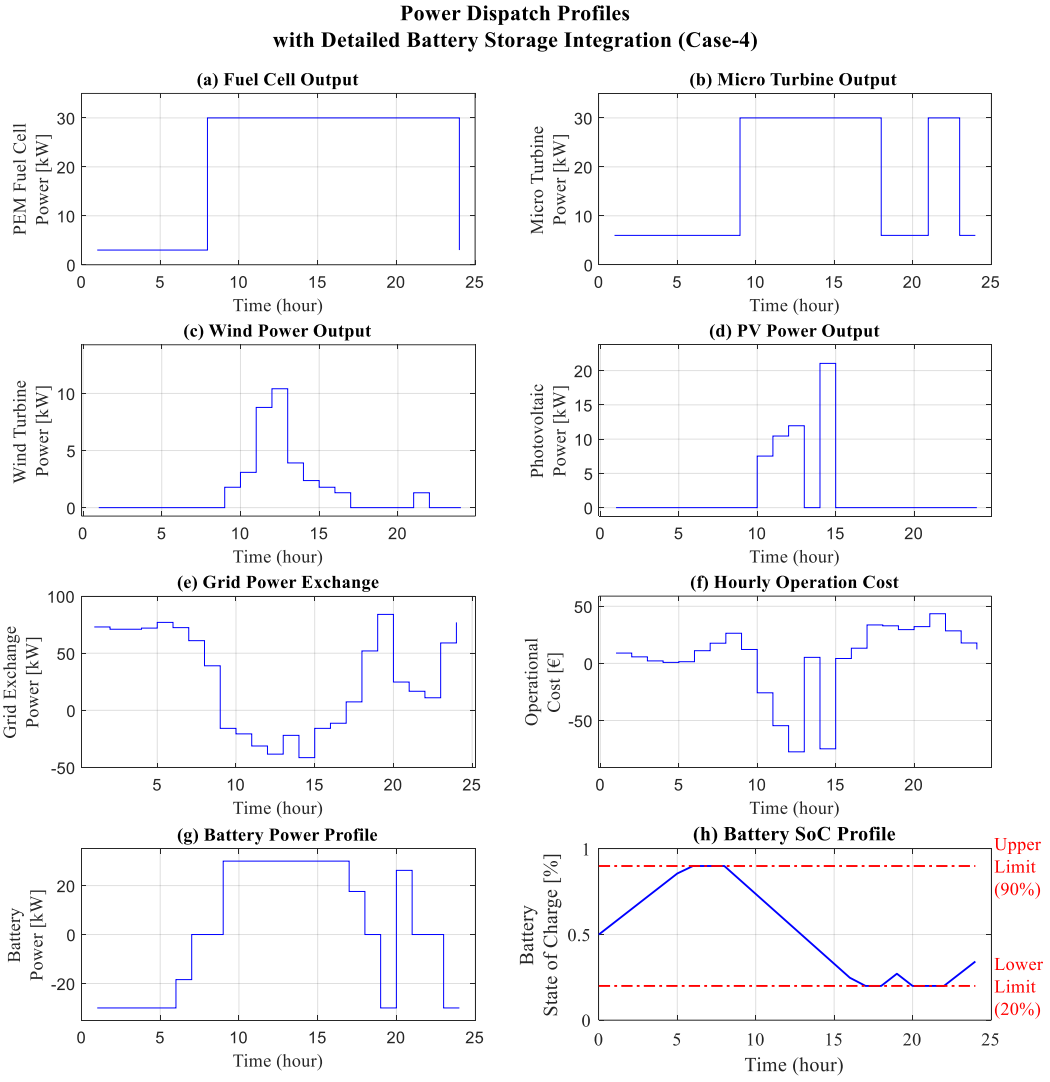

Fig. 6. 24-hour optimal power dispatch profiles considering detailed battery storage constraints (Case-4: Generation unit outputs a-FC, b-MT, c-WT, d-PV, e-Grid exchange power, f-Hourly operational cost, g-Battery power and h-Battery state of charge)

The evening operational pattern (17:00-24:00) showcases the system's ability to maintain stable and efficient operation. The battery system operates dynamically while strictly adhering to SoC limitations, facilitating balanced power exchange with the grid. This shows that there is effective coordination between all units of DERs. Thus, a good level is achieved in economic terms and system stability is also ensured.

The results obtained in this study demonstrate the importance of including realistic battery constraints in the operational planning of the MGs. It also highlights that storage system characteristics should be considered in cost

function calculations.

5. Conclusion

In this study, an optimization study is conducted using PFO algorithm for effective operation and management of MGs. In the study, cost minimization is considered as the objective function. This study presents a nonlinear optimization model for the optimal operation of MGs, considering both nonlinear objective functions and constraints. The use of a metaheuristic algorithm (Polar Fox Optimization) is justified by the complex and nonlinear nature of the problem, which cannot be effectively solved using traditional deterministic methods. The proposed approach provides a robust framework for handling the nonlinear interactions between distributed energy resources, storage systems, and grid exchange, ensuring both economic efficiency and system reliability. The study is conducted on four different scenarios. The effects on system performance and economics are investigated by modifying the constraints. In Case 1, it is assumed that all DERs are operating within the specified limits. In this case, all the energy produced by renewable DGs is injected into the MG. Case 1 served as a reference point for the other cases. As a result of the optimization study, the cost value is found to be €269.76/day. The value found is compatible with the literature. In Case 2, the output power of renewable DGs is accepted as the optimization variable. A 42.5% decrease in cost is occurred and the cost function is found to be 155.01 €/day. In case 3, the same conditions as in case 2 are valid. However, the utility power restriction (+30- and -30-kW limitation) is removed. The cost function for case 3 is calculated as 68.18 €/day. This result shows a reduction of 74.7% compared to the first case 1. Furthermore, the improvement in cost shows the impact of utility constraints on the operation costs and system efficiency. In Case 4, unlike the other cases, an optimization study was conducted by considering technical parameters such as battery efficiency, charge states, battery capacity and battery charge/discharge in order to solve the integration of the BES system to the grid with a more realistic approach. As a result of the study, the operating cost was calculated as 107.08 €/day. Although this cost is higher than the cost in Case 3, it allows the system to operate in a more realistic way since it takes into account practical battery limitations and battery efficiency.

This study shows the critical results obtained regarding the EOM of MGs. Firstly, optimizing the output power of renewable DGs contributed to the improvement of performance in economic terms. Secondly, removing constraints between MG and utility caused a significant decrease in costs. This situation showed the importance of grid infrastructure capacity. Thirdly, adding BESS constraints to the optimization with a realistic approach proved its importance for grid operation in daily life.

Future research can focus on enhancing the proposed optimization framework by incorporating multi-objective optimization to balance cost, environmental impact, and system resilience. Real-time optimization techniques using adaptive control and machine learning could improve decision-making under dynamic conditions. Additionally, integrating hybrid energy storage systems and exploring large-scale microgrid applications would enhance scalability and flexibility. Lastly, integrating the model with smart grid technologies, such as demand-side management and blockchain-based energy trading, could further optimize microgrid operations for sustainable and cost-effective energy management.

Acknowledgement

The author gratefully acknowledges the support provided by TÜBİTAK within the scope of the 1001 project under grant number 124E002.

Author Contribution

The writing of the manuscript and all analyses were conducted solely by the corresponding author.

Appendix A.

The following tables summarize the sets, indices, parameters, and decision variables used in the optimization framework.

A.1. Sets and indices

Symbol	Description
$t \in T$	Time periods (hours) in the planning horizon
$i \in I$	Set of distributed generation units
$s \in S$	Set of energy storage systems
$r \in R$	Set of renewable generation units (PV, WT)
X_i	Solution vector for i^{th} fox
X_{best}	Global best solution vector
X_{rand}	Randomly selected solution vector

A.2. Distributed/renewable power generation parameters

Symbol	Description	Unit
P_{MT}^{min} , P_{MT}^{max}	Min/max power output of microturbine	kW
P_{FC}^{min} , P_{FC}^{max}	Min/max power output of fuel cell	kW
P_{PV}^{max}	Maximum power output of PV system	kW
P_{WT}^{max}	Maximum power output of wind turbine	kW
P_{rated}	Rated power of battery system	kW
RD_{MT}, RU_{MT}	Ramp down/up rates of microturbine	kW/h
RD_{FC}, RU_{FC}	Ramp down/up rates of fuel cell	kW/h

A.3. Cost parameters

Symbol	Description	Unit
$\alpha_{FC}, \beta_{FC}, \gamma_{FC}$	Cost coefficients for fuel cell	€/kWh
a, b, c	Cost coefficients for microturbine	€/kWh
λt	Time-varying electricity price	€/kWh
C_{deg}	Battery degradation cost	€/kWh

A.4. Battery parameters

Symbol	Description	Unit
η_{charge}	Battery charging efficiency	%
$\eta_{discharge}$	Battery discharging efficiency	%
SoC_{min}	Minimum state of charge	%

SoC_{max}	Maximum state of charge	%
C_b	Battery capacity	kWh

A.5. Decision variables

Symbol	Description	Unit
$P_{MT}(t)$	Microturbine power output at time t	kW
$P_{FC}(t)$	Fuel cell power output at time t	kW
$P_{PV}(t)$	PV power output at time t	kW
$P_{WT}(t)$	Wind turbine power output at time t	kW
$P_b(t)$	Battery power (+ discharge, - charge) at time t	kW
$P_{grid}(t)$	Grid exchange power at time t	kW
SoC(t)	Battery state of charge at time t	%

References

[1] S. Mohammadi, B. Mozafari, S. Solimani, and T. Niknam, ‘‘An adaptive modified firefly optimisation algorithm based on hong's point estimate method to optimal operation management in a microgrid with consideration of uncertainties,’’ Energy, vol.51, pp.339-348, March. 2013, doi: 10.1016/j.energy.2012.12.013.
[2] M. Cikan and N. N.Cikan, ‘‘Optimum allocation of multiple type and number of DG units based on IEEE 123-bus unbalanced multi-phase power distribution system’’ International Journal of Electrical Power & Energy Systems, vol.144, pp.1-17, Jan. 2023, doi: 10.1016/j.ijepes.2022.108564.
[3] M. Çıkan, “Çita optimizasyon algoritması kullanarak kısmi gölgelenme altındaki fotovoltaik sistemlerde maksimum güç noktası izleyicisinin tasarlanması,” Gazi Üniversitesi Mühendislik Mimarlık Fakültesi Dergisi, vol.40, no.1, pp. 555–572, Jan. 2025, doi: 10.17341/gazimmfd.1183267.
[4] M. Çıkan and N.N. Çıkan, ‘‘Elektrikli araç şarj istasyonlarının enerji dağıtım hatlarına optimum şekilde konumlandırılması’’ Kahramanmaraş Sütçü İmam Üniversitesi Mühendislik Bilimleri Dergisi, vol.27, no.2, pp. 340-363, Jun. 2024, doi:10.17780/ksujes.1365209.
[5] M.Cikan, N.N. Cikan, B. Kekezoglu, “Determination of optimal island regions with simultaneous DG allocation and reconfiguration in power distribution networks,” IET Renewable Power Generation, vol.19, pp. e12942, 2025, doi:10.1049/rpg2.12942.
[6] C. Marnay, N. DeForest and J. Lai, “A green prison: The Santa Rita Jail campus microgrid,’’ IEEE Power and Energy Society General Meeting, 2012, pp.1-2, doi: 10.1109/PESGM.2012.6345235.
[7] T. Gabderakhmanova et al., “Demonstrations of DC Microgrid and Virtual Power Plant Technologies on the Danish Island of Bornholm,’’ 55th International Universities Power Engineering Conference (UPEC), 2020, pp. 1-6, doi: 10.1109/UPEC49904.2020.9209853.
[8] S. Ahmad, M. Shafiullah, C. B. Ahmed and M. Alowaifeer, “A Review of Microgrid Energy Management and Control Strategies,’’ IEEE Access, vol. 11, pp. 21729-21757, 2023, doi: 10.1109/ACCESS.2023.3248511
[9] N.N. Cikan and M. Cikan, ‘‘Reconfiguration of 123-bus unbalanced power distribution network analysis by considering minimization of current & voltage unbalanced indexes and power loss,’’ International Journal of Electrical Power & Energy Systems, vol.157, pp.1-15, Jun.2024, doi: 10.1016/j.ijepes.2024.109796.
[10] M. Cikan and B. Kekezoglu, ‘‘Comparison of metaheuristic optimization techniques including Equilibrium optimizer algorithm in power distribution network reconfiguration,’’ Alexandria Engineering Journal, vol.61, no.2, pp. 991-1031, Feb. 2022, doi: 10.1016/j.aej.2021.06.079.
[11] K. Doğanşahin and M. Çıkan, ‘‘A new line stability index for voltage stability analysis based on line loading,’’ Clean Energy Technologies Journal, vol.1, no.1, pp.23-30, 2023.
[12] A. Mortazavi, “Comparative assessment of five metaheuristic methods on distinct problems,” Dicle Üniversitesi Mühendislik Fakültesi Mühendislik Dergisi (DUJE), vol. 10, pp. 879–898, 2019, doi: 10.24012/dumf.585790.
[13] A. Mortazavi, “A fuzzy reinforced Jaya algorithm for solving mathematical and structural optimization problems,’’ Soft Computing, vol. 28, pp. 2181–2206, 2024, doi:10.1007/s00500-023-09206-5.
[14] A. Akter et al., ‘‘A review on microgrid optimization with meta-heuristic techniques: Scopes, trends and recommendation,’’ Energy Strategy Reviews, vol. 51, pp. 1-27, Jan. 2024, doi: 10.1016/j.esr.2024.101298.
[15] S. Phommixay, M.L. Doumbia, and D. Lupien St-Pierre, ‘‘Review on the cost optimization of microgrids via particle swarm optimization,’’ International Journal of Energy and Environmental Engineering, vol. 11, pp. 73-89, 2020, doi: 0.1007/s40095-019-00332-1.
[16] M. A. Hossain, H. R. Pota, S. Squartini, F. Zaman, and K.M. Muttaqi, ‘‘Energy management of community microgrids considering degradation cost of battery,’’ Journal of Energy Storage, vol.22, pp.257-269, April 2019, doi: 10.1016/j.est.2018.12.021.
[17] S. Sharma, S. Bhattacharjee, and A. Bhattacharya, ‘‘Probabilistic operation cost minimization of Micro-Grid,’’ Energy, vol.148, pp. 1116-1139, 2018, doi: 10.1016/j.energy.2018.01.164.

[18] Z. Zheng, S.Yang, Y. Guo, X. Jin, and R. Wang, "Meta-heuristic Techniques in Microgrid Management: A Survey'' Swarm and Evolutionary Computation, vol.78, pp.101256, 2023, doi: 10.1016/j.swevo.2023.101256.
[19] A. Mortazavi, "Marathon runner algorithm: theory and application in mathematical, mechanical and structural optimization problems,'' Materials Testing, vol. 66, pp. 1267-1291,2024, doi: 10.1515/mt-2023-009.
[20] M. Moloodpoor, A. Mortazavi, and N. Ozbalta, "Thermo-economic optimization of double-pipe heat exchanger using a compound swarm intelligence,'' Heat Transfer Research, vol.52, pp.1-20,2021, doi: 10.1615/HeatTransRes.2021037293.
[21] E. C. Kandemir, and A. Mortazavi, "Optimization of Seismic Base Isolation System Using a Fuzzy Reinforced Swarm Intelligence,'' Advances in Engineering Software, vol.174, pp. 103323, 2022, doi: 10.1016/j.advengsoft.2022.103323.
[22] M. Cikan, and K. Dogansahin, "A Comprehensive Evaluation of Up-to-Date Optimization Algorithms on MPPT Application for Photovoltaic Systems," Energy Sources, Part A: Recovery, Utilization, and Environmental Effects, vol.45, pp.10381–10407, 2023, doi:10.1080/15567036.2023.2245771.
[23] N.N. Cikan, "Optimization of PV, Capacitor Bank, and EV Charging Station Allocation in a 33-Bus Power Distribution System Using the Slime Mould Algorithm" European Journal of Engineering and Natural Sciences (EJENS), vol.9, pp.55-60, 2024.
[24] N.N. Cikan, "Optimization of a 33-Bus Power Distribution System Using Artificial Hummingbird Algorithm for Power Loss and Voltage Stability Enhancement," European Journal of Engineering and Natural Sciences (EJENS), vol.9, pp.41-46, 2024.
[25] M.Gendreau, and JY. Potvin, "Metaheuristics in Combinatorial Optimization,'' Annals of Operation Research, vol. 140, pp.189–213, 2005, doi:10.1007/s10479-005-3971-7.
[26] I. Boussaïd, J. Lepagnot, and P. Siarry, "A survey on optimization metaheuristics,'' Information Sciences, vol. 237, pp.82-117, 2013, doi: 10.1016/j.ins.2013.02.041.
[27] S. Yang, Y. Jiang, and T.T. Nguyen, "Metaheuristics for dynamic combinatorial optimization problems,'' IMA Journal of Management Mathematics, vol.24, pp.451–480, 2013, doi: 10.1093/imaman/dps021.
[28] C. Gamarra, and J. M. Guerrero, "Computational optimization techniques applied to microgrids planning: A review,'' Renewable and Sustainable Energy Reviews, vol. 48, pp. 413-424, 2015, doi: 10.1016/j.rser.2015.04.025.
[29] M. F. Zia, E. Elbouchikhi, and M. Benbouzid, "Microgrids energy management systems: A critical review on methods, solutions, and prospects,'' Applied Energy, vol. 222, pp. 1033-1055, 2018, doi: 10.1016/j.apenergy.2018.04.103.
[30] T. Niknam, F. Golestaneh, and A. Malekpour, ''Probabilistic energy and operation management of a microgrid containing wind/photovoltaic/fuel cell generation and energy storage devices based on point estimate method and self-adaptive gravitational search algorithm,'' Energy, vol.43, no.1, pp. 427-437, July 2012, 10.1016/j.energy.2012.03.064.
[31] A. Ghiaskar, A. Amiri, S. Mirjalili, ''Polar fox optimization algorithm: a novel meta-heuristic algorithm,'' Neural Computing and Applications, vol.36, pp. 20983–21022, Aug. 2024, doi: 10.1007/s00521-024-10346-4.
[32] J. Radosavljevic, ''Optimal energy and operation management of microgrids,'' in Metaheuristic Optimization in Power Engineering, 1st ed. London, England: IET, ch.12, pp. 407-447.
[33] H. Saadat, Power system analysis. New York, NY, USA: McGraw-Hill,1999.
[34] J. Radosavljevic, ''Optimal power flow in transmission networks,'' in Metaheuristic Optimization in Power Engineering, 1st ed. London, England: IET, ch.6, pp. 177-233.
[35] S. Mohammadi, S. Soleymani, and B. Mozafari, ''Scenario-based stochastic operation management of microgrid including wind, photovoltaic, micro-turbine, fuel cell and energy storage devices,'' International Journal of Electrical Power & Energy Systems, vol. 54, pp.525-535, Jan.2014, doi: 10.1016/j.ijepes.2013.08.004.
[36] A. A. Moghaddam, A. Seifi, T. Niknam, and M. R. A. Pahlavani, ''Multi-objective operation management of a renewable MG (micro-grid) with back-up micro-turbine/fuel cell/battery hybrid power source,'' Energy, vol.36, no.11, pp. 6490-6507, Nov.2011, doi: 10.1016/j.energy.2011.09.017.